Article

Design of Amino Acid Aldehydes as Transition-State Analogue Inhibitors of Arginase

Hyunshun Shin, Evis Cama, and David W. Christianson

J. Am. Chem. Soc., **2004**, 126 (33), 10278-10284• DOI: 10.1021/ja047788w • Publication Date (Web): 30 July 2004

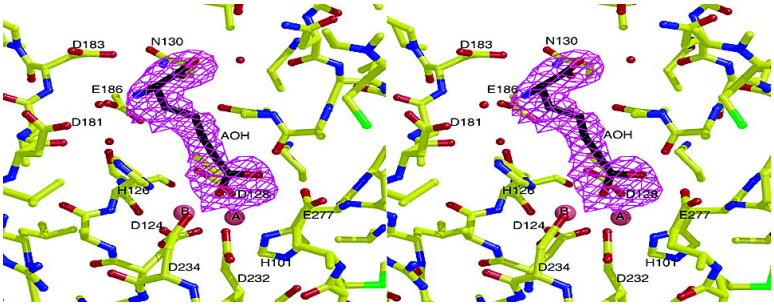

More About This Article

Additional resources and features associated with this article are available within the HTML version:

- Supporting Information
- Access to high resolution figures
- Links to articles and content related to this article
- Copyright permission to reproduce figures and/or text from this article

View the Full Text HTML

J|A|C|S
ARTICLES
Published on Web 07/30/2004

Design of Amino Acid Aldehydes as Transition-State Analogue Inhibitors of Arginase

Hyunshun Shin, Evis Cama, and David W. Christianson*

Contribution from the Roy and Diana Vagelos Laboratories, Department of Chemistry, University of Pennsylvania, Philadelphia, Pennsylvania 19104-6323

Received April 16, 2004; E-mail: chris@xtal.chem.upenn.edu

Abstract: Arginase is a binuclear manganese metalloenzyme that catalyzes the hydrolysis of L-arginine to form L-ornithine and urea. Chiral L-amino acids bearing aldehyde side chains have been synthesized in which the electrophilic aldehyde C=O bond is isosteric with the C=N bond of L-arginine. This substitution is intended to facilitate nucleophilic attack by the metal-bridging hydroxide ion upon binding to the arginase active site. Syntheses of the amino acid aldehydes have been accomplished by reduction, oxidation, and Wittig-type reaction with a commercially available derivative of L-glutamic acid. Amino acid aldehydes exhibit inhibition in the micromolar range, and the X-ray crystal structure of arginase I complexed with one of these inhibitors, (*S*)-2-amino-7-oxoheptanoic acid, has been determined at 2.2 Å resolution. In the enzyme−inhibitor complex, the inhibitor aldehyde moiety is hydrated to form the gem-diol: one hydroxyl group bridges the Mn^{2+}_2 cluster and donates a hydrogen bond to D128, and the second hydroxyl group donates a hydrogen bond to E277. The binding mode of the neutral gem-diol may mimic the binding of the neutral tetrahedral intermediate and its flanking transition states in arginase catalysis.

Introduction

Arginase is a 105-kD trimeric metalloenzyme that catalyzes the hydrolysis of L-arginine to form L-ornithine and urea, and two mammalian isozymes have been identified.[1−3] Arginase I catalyzes the final cytosolic step of the urea cycle in the liver, whereas arginase II is nonhepatic and functions predominantly in L-arginine homeostasis. The X-ray crystal structures of rat arginase I and human arginase II, as well as the hexameric arginase from *Bacillus caldovelox*, reveal a binuclear manganese cluster located at the base of a ∼15 Å-deep active site cleft.[4−6] The pH−rate profile[7] of arginase I exhibits an activity-linked pK_a of 7.9, consistent with the ionization of the likely catalytic nucleophile, a metal-bridging solvent molecule.[4] Structure−activity relationships outlined for site-specific variants of arginase I are consistent with a metal-activated hydroxide mechanism in which the metal-bridging hydroxide ion attacks the substrate guanidinium group oriented by hydrogen bonds with E277 and the backbone carbonyl of H141 (Figure 1).[4,8]

On the basis of Hammond's postulate,[9] the transition state for the nucleophilic attack of hydroxide ion at the guanidinium carbon is expected to be close in structure and energy to the metastable tetrahedral intermediate illustrated in Figure 1, and this has motivated the investigation of tetrahedral transition-state analogues. For example, in a recent study we reported the X-ray crystal structure of arginase I complexed with an amino acid sulfonamide: the NH_2 group of the tetrahedral sulfonamide ionizes to the NH− form, which bridges the binuclear manganese cluster and donates a hydrogen bond to D128.[10] In earlier work, we reported boronic acid analogues of L-arginine in which the trigonal planar boronic acid moiety is substituted for the trigonal planar guanidinium group.[11,12] Strictly speaking, these boronic acid analogues are substrate analogues and not transition-state analogues. However, the electron-deficient boron atom in each of these analogues facilitates nucleophilic attack by hydroxide ion to form a tetrahedral boronate anion.[5,12,13] Accordingly, boronic acid inhibitors of arginase are reactive substrate analogues that, upon binding to the enzyme, undergo a chemical transformation to better mimic the tetrahedral intermediate and its flanking transition states in catalysis. Since this chemical transformation mimics the first bond-making step with an actual substrate, such reactive substrate analogues have been designated "reaction coordinate analogues".[14] The chemical

* Corresponding author: phone 215-898-5714; fax 215-573-2201.

(1) Christianson, D. W.; Cox, J. D. *Annu. Rev. Biochem.* **1999**, *68*, 33−57.
(2) Ash, D. E.; Cox, J. D.; Christianson, D. W. *Metal Ions in Biological Systems*; Sigel, A., Sigel, H., Eds.; M. Dekker: New York, 2000; Vol. 37 (Manganese and its Role in Biological Processes), pp 408−428.
(3) Morris, S. M., Jr. *Annu. Rev. Nutr.* **2002**, *22*, 87−105.
(4) Kanyo, Z. F.; Scolnick, L. R.; Ash, D. E.; Christianson, D. W. *Nature* **1996**, *383*, 554−557.
(5) Cama, E.; Colleluori, D. M.; Emig, F. A.; Shin, H.; Kim, S. W.; Kim, N. N.; Traish, A. M.; Ash, D. E.; Christianson, D. W. *Biochemistry* **2003**, *42*, 8445−8451.
(6) Bewley, M. C.; Jeffrey, P. D.; Patchett, M. L.; Kanyo, Z. F.; Baker, E. N. *Structure* **1999**, *7*, 435−448.
(7) Kuhn, N. J.; Talbot, J.; Ward, S. *Arch. Biochem. Biophys.* **1991**, *286*, 217−221.
(8) Cama, E.; Emig, F. A.; Ash, D. E.; Christianson, D. W. *Biochemistry* **2003**, *42*, 7748−7758.
(9) Hammond, G. S. *J. Am. Chem. Soc.* **1955**, *77*, 334−338.
(10) Cama, E.; Shin, H. S.; Christianson, D. W. *J. Am. Chem. Soc.* **2003**, *125*, 13052−13057.
(11) Baggio, R.; Elbaum, D.; Kanyo, Z. F.; Carroll, P. J.; Cavalli, R. C.; Ash, D. E.; Christianson, D. W. *J. Am. Chem. Soc.* **1997**, *119*, 8107−8108.
(12) Kim, N. N.; Cox, J. D.; Baggio, R. F.; Emig, F. A.; Mistry, S.; Harper, S. L.; Speicher, D. W.; Morris, S. M., Jr.; Ash, D. E.; Traish, A. M.; Christianson, D. W. *Biochemistry* **2001**, *40*, 2678−2688.
(13) Cox, J. D.; Kim, N. N.; Traish, A. M.; Christianson, D. W. *Nat. Struct. Biol.* **1999**, *6*, 1043−1047.

10.1021/ja047788w CCC: $27.50

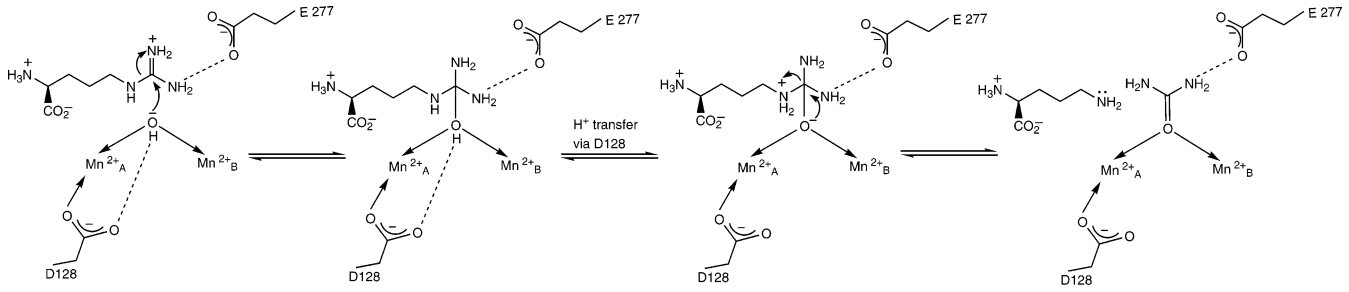

Figure 1. Proposed mechanism of arginase.

Scheme 1. Synthesis of (*S*)-2-Amino-7-oxoheptanoic Acid

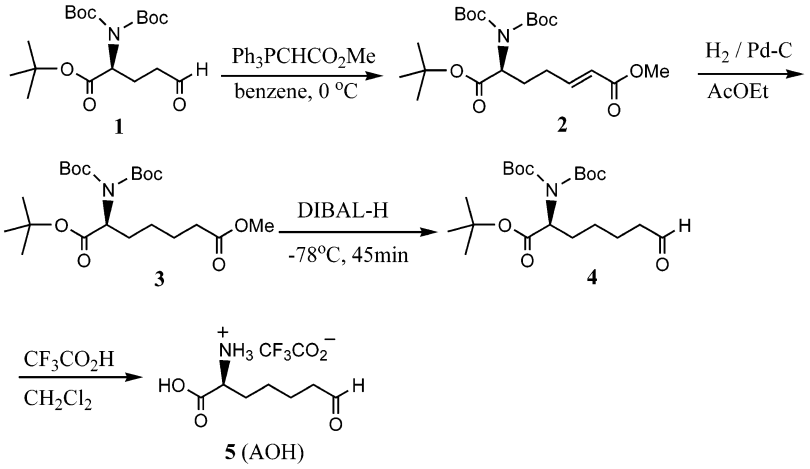

Scheme 2. Synthesis of (*S*)-(*E*)-2-Amino-7-oxohept-5-enoic Acid

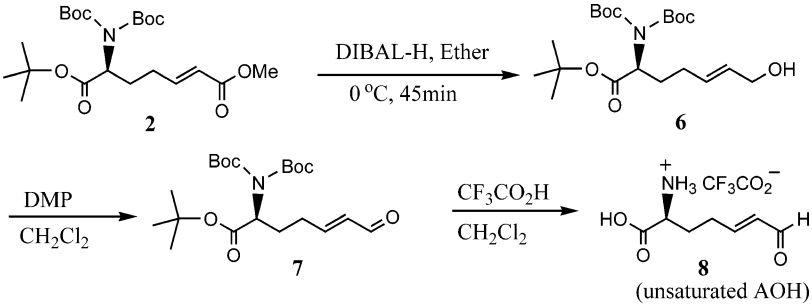

reactivity of a reaction coordinate analogue exploits the tendency of an enzyme to bind the transition state (or transition-state analogue) more tightly than the substrate (or substrate analogue).[15]

Compounds containing the aldehyde moiety can similarly serve as reaction coordinate analogues for hydrolytic enzymes due to the enhanced susceptibility of the aldehyde carbonyl to nucleophilic attack. Like the electron-deficient boronic acid, a properly oriented aldehyde group in a metalloenzyme inhibitor can undergo nucleophilic attack by a metal-bound solvent molecule to form a tetrahedral gem-diol. Aldehyde moieties have been incorporated into inhibitors of the zinc proteases leucine aminopeptidase and carboxypeptidase A,[16−18] and the crystal structures of these enzyme−inhibitor complexes confirm the binding of each inhibitor as a gem-diol in its target enzyme active site.[19,20]

Given the successful incorporation of the aldehyde moiety into inhibitors of the zinc proteases,[16−20] we hypothesized that the substitution of the trigonal planar aldehyde moiety for the trigonal planar guanidinium group of L-arginine would yield a reactive substrate analogue capable of binding as a gem-diol analogue of the tetrahedral intermediate in the arginase mechanism. Here, we report the design and synthesis of two amino acid aldehyde inhibitors of arginase: (*S*)-2-amino-7-oxoheptanoic acid (AOH; **5**, Scheme 1) and (*S*)-(*E*)-2-amino-7-oxohept-5-enoic acid (unsaturated AOH; **8**, Scheme 2). The X-ray crystal structure of the arginase I−AOH complex reveals that, as designed, the inhibitor binds to the enzyme active site as the tetrahedral gem-diol.

Experimental Section

Syntheses of Amino Acid Aldehydes. Reactions requiring anhydrous conditions were carried out under a nitrogen atmosphere in flame- or oven-dried glassware, and solvents were freshly distilled. Diethyl

(14) Christianson, D. W.; Lipscomb, W. N. *Acc. Chem. Res.* **1989**, *22*, 62−69.
(15) Pauling, L. *Chem. Eng. News* **1946**, *24*, 1375−1377.
(16) Andersson, L.; Isley, T. C.; Wolfenden, R. *Biochemistry* **1982**, *21*, 4177−4180.
(17) Andersson, L.; MacNeela, J.; Wolfenden, R. *Biochemistry* **1985**, *24*, 330−333.
(18) Galardy, R. E.; Kortylewicz, Z. P. *Biochemistry* **1984**, *23*, 2083−2087.
(19) Christianson, D. W.; Lipscomb, W. N. *Proc. Natl. Acad. Sci. U.S.A.* **1985**, *82*, 6840−6844.
(20) Sträter, N.; Lipscomb, W. N. *Biochemistry* **1995**, *34*, 14792−14800.

ether and tetrahydrofuran (THF) were distilled from sodium/benzophenone. Dichloromethane and triethylamine were distilled from calcium hydride. Benzene was dried with molecular sieves. Ethyl acetate was dried by passage through a column of alumina. All other reagents and solvents were used without further purification from commercial sources. Organic extracts were dried over $MgSO_4$ or Na_2SO_4. Reactions were monitored by thin-layer chromatography (TLC) with 0.25-mm E. Merck precoated silica gel plates and visualized with ninhydrin solution (0.1% ninhydrin in 95% *n*-butanol, 4.5% water, 0.5% glacial acetic acid) and $KMnO_4$ solution (3 g of $KMnO_4$, 20 g of K_2CO_3, 5 mL of 5% NaOH, and 300 mL of water). Flash column chromatography was carried out with E. Merck silica gel 60 (230−240 mesh ASTM). The ^1H and ^{13}C NMR spectra were recorded on a Bruker AM-500 spectrometer. Chemical shifts were expressed in parts per million (ppm) and referenced to $CDCl_3$, CD_3OD, or DMSO-d_6. The general syntheses of (*S*)-2-amino-7-oxoheptanoic acid **5** and (*S*)−(*E*)-2-amino-7-oxohept-5-enenoic acid **8** are as follows.

(*S*)-(*E*)-1-*tert*-Butyl-[*bis*-(2-*tert*-butoxycarbonyl)amino]-7-methyl-hept-5-eneoate, 2. To a stirred solution of (*S*)-1-*tert*-butyl-[bis(2-*tert*-butoxycarbonyl)amino]-5-oxopentanoate **1** (2.8 g, 7.23 mmol) in benzene (25 mL) was added commercially available methyl (triphenylphosphoranylidene)acetate (4.8 g, 14.46 mmol) at 0 °C. The mixture was stirred until TLC showed the complete consumption of the starting material. The solvent was removed on a rotary evaporator, and the crude residue was purified by silica gel chromatography to yield **2** (2.2 g, 79% yield). ^1H NMR ($CDCl_3$): δ 6.95−6.89 (m, 1H), 5.81 (d, J = 15.6 Hz, 1H), 4.75−4.59 (m, 1H), 3.69 (s, 3H), 2.27−2.21 (m, 3H), 2.21−1.96 (m, 1H), 1.45 (s, 18H), 1.41 (s, 9H). ^{13}C NMR ($CDCl_3$): δ 169.4, 166.9, 152.4, 148.1, 121.6, 82.9, 81.4, 58.3, 51.4, 29.1, 28.0, 27.93, 27.8. HRMS (EI) (*m*/*z*): [M+] calcd for $C_{22}H_{37}O_8N$, 443.2417; found, 443.2430.

(*S*)-1-*tert*-Butyl-[*bis*-(2-*tert*-butoxycarbonyl)amino]-7-methyl-heptanoate, 3. To a stirred solution of **2** (0.96 g, 2.16 mmol) in dry EtOAc (20 mL) was added Pd/C (90 mg). The reaction was stirred under hydrogen atmosphere until TLC showed the complete conversion of starting material. The mixture was filtered through a pad of Celite. The solvent was removed on a rotary evaporator, and the crude residue was purified by silica gel chromatography to yield **3** (0.91 g, 95% yield). ^1H NMR ($CDCl_3$): δ 4.67−4.64 (m, 1H), 3.63 (s, 3H), 2.27 (t, J = 7.7 Hz, 2H), 2.05−1.98 (m, 1H), 1.86−1.78 (m, 1H), 1.68−1.52 (m, 4H), 1.46 (s, 18H), 1.40 (s, 9H). ^{13}C NMR ($CDCl_3$): δ 173.9, 169,8, 152.4, 82.66, 81.1, 58.7, 51.4, 33.9, 28.9, 28.0, 27.9, 26.0, 24.6. MS (ES+) (*m*/*z*): [M+] calcd for ($C_{22}H_{39}O_8N$) 445.27; found, 445.60.

(*S*)-1-*tert*-Butyl-[*bis*-(2-*tert*-butoxycarbonyl)amino]-7-oxo-heptanoate, 4. To a stirred solution of **3** (0.91 g, 2.0 mmol) in dry ether (20 mL) was added dropwise DIBAL-H (3.5 mL, 1.0 M in hexane, 3.0 mmol) to −78 °C. The reaction was stirred for 45 min. It was quenched with H_2O (0.25 mL, 7 equiv) and allowed to warm to room temperature. The mixture was stirred for 30 min, dried over $MgSO_4$, and filtered through a pad of Celite. The solvent was removed on a rotary evaporator, and the crude residue was purified by silica gel chromatography to yield **4** (0.80 g, 95% yield). ^1H NMR ($CDCl_3$): δ 9.73 (s, 1H), 4.69−4.65 (m, 1H), 2.42−2.39 (m, 2H), 2.08−2.02 (m, 1H), 1.86−1.82 (m, 1H), 1.69−1.29 (m, 4H), 1.45 (s, 18H), 1.41 (s, 9H). ^{13}C NMR ($CDCl_3$): δ 202.4, 169.8, 152.5, 82.8, 81.2, 58.6, 43.7, 30.0, 28.0, 26.0, 21.8. MS (ES+) (*m*/*z*): [M+] calcd for ($C_{21}H_{37}O_7N$) 415.26; found, 415.54.

(*S*)-2-Amino-7-oxoheptanoic Acid, 5. To a stirred solution of **4** (0.1 g, 0.24 mmol) in CH_2Cl_2 (1 mL) at 0 °C was slowly added trifluoroacetic acid (TFA) (1 mL). The reaction mixture was stirred for 15 min at 0 °C and then allowed warm to room temperature until the end of the reaction. The solvent was removed on a rotary evaporator, and the crude residue was purified by silica gel chromatography to yield **5** (0.041 g, 63% yield). ^1H NMR (CD_3OD): δ 9.36 (s, 1H), 3.97−3.93 (m, 1H), 2.3−1.9 (m, 2H), 1.59−1.27 (m, 6H). MS (ES+) (*m*/*z*): [M+] calcd for ($C_7H_{13}O_3N$) 159.08; found, 159.06.

(*S*)-(*E*)-1-*tert*-Butyl-[*bis*-(2-*tert*-butoxycarbonyl)amino]-7-hydroxy-hept-5-eneoate, 6. To a stirred solution of **2** (1.4 g, mmol) in dry ether (10 mL) was added dropwise DIBAL-H (7.9 mL, 1.0 M in hexane, 7.9 mmol) at 0 °C. The reaction mixture was stirred for 1 h. It was quenched with H_2O (0.56 mL) and allowed to warm to room temperature. The mixture was stirred for 30 min, dried over $MgSO_4$, and filtered through a pad of Celite. The solvent was removed on a rotary evaporator, and the crude residue was purified by silica gel chromatography to yield **6** (1.0 g, 77% yield). ^1H NMR ($CDCl_3$): δ 5.67−5.58 (m, 2H), 4.75−4.72 (m, 1H), 4.03 (dd, J = 5.5, 2.0 Hz, 2H), 2.30−2.08 (m, 3H), 1.97−1.90 (m, 1H), 1.47 (s, 18H), 1.41 (s, 9H). ^{13} C NMR ($CDCl_3$): δ 169.8, 152.5, 132.3, 130.1, 82.7, 81.2, 63.8, 58.3, 29.1, 27.3. MS (ES+) (*m*/*z*): [M+] calcd for ($C_{21}H_{37}O_7N$) 415.26; found, 415.54.

(*S*)-(*E*)-1-*tert*-Butyl-[*bis*-(2-*tert*-butoxycarbonyl)amino]-7-oxo-hept-5-enoate, 7. A solution of **6** (0.59 g, 1.43 mmol) in CH_2Cl_2 (20 mL) was added to Dess−Martin periodinane (3.6 mL, 1.71 mmol, 15 wt % in CH_2Cl_2) at 0 °C. Stirring was continued at 0 °C for 15 min, followed by warming to ambient temperature. The reaction was monitored by TLC. After 1 h the mixture was diluted with diethyl ether (30 mL), poured into 40 mL of ice-cold saturated $NaHCO_3$/saturated $Na_2S_2O_3$ (1:1), and shaken for 5 min. The organic phase was separated and washed with saturated $NaHCO_3$, H_2O, and saturated NaCl, dried over Na_2SO_4, and concentrated in vacuo. The residue was purified by chromatography to afford **7** (0.348 g, 60% yield). ^1H NMR ($CDCl_3$): δ 9.50 (d, 1H), 6.81−6.57 (m, 1H), 6.12−6.07 (m, 1H), 4.73−4.69 (m, 1H), 2.63−2.24 (m, 3H), 2.05−1.99 (m, 1H), 1.47 (s, 18H), 1.41 (s, 9H). MS (ES+) (*m*/*z*): [M + Na] calcd for ($C_{21}H_{35}O_7N$+Na) 436.22; found 436.60, isotope 437.60.

(*S*)-(*E*)-2-Amino-7-oxo-hept-5-enoic Acid, 8. To a stirred solution of **7** (0.425 g, 1.03 mmol) in CH_2Cl_2 (8 mL) was slowly added TFA (8 mL) at 0 °C. The reaction mixture was stirred for 15 min and then allowed to equilibrate at room temperature until the end of the reaction. The solvent was removed on a rotary evaporator, and the crude residue was purified by silica gel chromatography to yield **8** (0.24 g, 87% yield). ^1H NMR (CD_3OD): δ 9.01 (s, 1H), 6.94−6.91 (m, 1H), 5.91−5.88 (d, J = 16 Hz, 1H), 3.97−3.95 (m, 1H), 2.50−1.90 (m, 4H). MS (ES+) (*m*/*z*): [M+] calcd for ($C_7H_{11}O_3N$) 157.07, found 157.86.

Kinetic Assays. Arginase inhibition by AOH was evaluated using a modified version of the fixed-point radioactive assay developed by Rüegg and Russell.[21] Assay mixtures contained 500 μL of CHES−NaOH (100 mM, pH 9.5), 100 μL of 1 mM $MnCl_2$, 10 μL of 0.05 μCi of [^{14}C-guanido]-L-arginine, 90 μL of water, 100 μL of 100 mM unlabeled L-arginine, then taking 40 μL of the assay mixtures and 5 μL of varying concentrations of AOH in a 50 μL volume per centrifuge tube. Reactions were started by the addition of 5 μL of a 10 μg/mL wild-type arginase I solution. After 5 min, reactions were quenched by the addition of 400 μL of "stop" solution (0.25 mM acetic acid (pH 4.5), 7 M urea, 10 mM L-arginine, and a 1:1 (v/v) slurry of Dowex W−X8 in water). Each reaction mixture was vortexed immediately after the addition of "stop" solution, gently mixed for an additional 5 min, and centrifuged at 6000 rpm for 10 min. A 200 μL volume of the supernatant was removed, and 3 mL of scintillation liquid (EcoScint) was added in preparation for liquid scintillation counting in a Beckman counter (model LS 6000 SC). For data analysis, the plot of v_o/v as a function of inhibitor concentration was expected to be linear for a simple competitive inhibitor, and the slope of the line was used to calculate K_i using the equation for competitive binding (v_o and v were the observed velocities measured in the absence and presence of inhibitor, respectively).

Crystallography. For ease of protein handling, a multisite-specific variant of rat arginase I was utilized for the preparation of the enzyme−inhibitor complex. Crystals of this variant consistently diffracted to higher resolution than crystals of the wild-type enzyme. The C119A/

(21) Rüegg, U. T.; Russell, A. S. *Anal. Biochem.* **1980**, *102*, 206−212.

Table 1. Data Collection and Refinement Statistics

resolution (Å)	2.2
total reflections (*N*)	123 870
unique reflections (*N*)	43 716
completeness (%) (last shell)	93.0 (85.4)[a]
R_{merge} (last shell)[b]	0.080 (0.327)[a]
reflections used in refinement (test set)[c]	41 783 (2099)[a]
R_{cryst}[c]	0.222
R_{free}[c]	0.241
rms deviations	
bonds (Å)	0.015
angles (deg)	2.1
dihedrals (deg)	24.0
impropers (deg)	1.0
R_{cryst}[c]	0.222

[a] Numbers in parentheses refer to the outer 0.1 Å shell of data. [b] R_{merge} for replicate reflections, $R = \Sigma|I_{\mathbf{h}} - \langle I_{\mathbf{h}}\rangle|/\Sigma\langle I_{\mathbf{h}}\rangle$; $I_{\mathbf{h}}$ = intensity measured for reflection **h**; $\langle I_{\mathbf{h}}\rangle$ = average intensity for reflection **h** calculated from replicate data. [c] Crystallographic *R* factor, $R_{cryst} = \Sigma||\boldsymbol{F}_o| - |\boldsymbol{F}_c||/\Sigma|\boldsymbol{F}_o|$ for reflections contained in the working set. Free *R* factor, $R_{free} = \Sigma||\boldsymbol{F}_o| - |\boldsymbol{F}_c||/\Sigma|\boldsymbol{F}_o|$ for reflections contained in the test set held aside during refinement (5% of total). $|\boldsymbol{F}_o|$ and $|\boldsymbol{F}_c|$ are the observed and calculated structure factor amplitudes, respectively.

C168A/C303A/H141A/Q19C variant was prepared by site-directed mutagenesis as described.[22] The plasmid was then transformed into *E. coli* BL21(DE3) cells and purified by the same procedure utilized for the purification of recombinant wild-type arginase. Finally, the variant was chemically modified at C19 with 3-bromopropylamine and accordingly designated BPA-arginase I. Activity assays of BPA-arginase I yield K_M and k_{cat} values of 0.4 mM and 0.55 s^{-1}, respectively, indicating 0.22% of wild-type activity.[22] Since neither the binuclear manganese cluster nor the nucleophilic metal-bridging hydroxide ion is perturbed in BPA-arginase I, the reactivity of the metal-bridging hydroxide ion is not compromised.

The BPA arginase I variant was crystallized using the hanging drop vapor diffusion method, as achieved for the native rat liver enzyme.[23] Briefly, a 3 μL drop of precipitant solution [50 mM bicine (pH 8.2−8.5), 20−24% PEG 8000, 2−5 mM $MnCl_2$] was added to a 3 μL drop of protein solution [10−16 mg/mL BPA arginase I variant, 50 mM bicine (pH 8.5), 100 μM $MnCl_2$] on a silanized cover slip subsequently inverted and sealed over a 1 mL reservoir of precipitant buffer at 4 °C. Crystals appeared after 4 weeks and were nearly isomorphous with those of the wild-type enzyme.[4,23] Crystals belonged to space group $P3_2$ with unit cell parameters $a = b = 87.9$ Å, $c = 105.2$ Å. Data collection statistics are recorded in Table 1. The BPA arginase I−AOH complex was prepared by soaking enzyme crystals for 3−8 days in 26% PEG 8000, 100 mM bicine (pH 8.5), 3 mM $MnCl_2$, and 5 mM AOH. Prior to data collection, crystals were gradually transferred to a cryoprotectant solution consisting of the original precipitant solution plus 30% glycerol and then flash-cooled with liquid nitrogen.

X-ray diffraction data were collected at the Advance Light Source, beamline 5.0.1. Intensity data integration and reduction were performed using the HKL suite of programs.[24] Initial phases were determined by molecular replacement with AmoRe[25,26] using the structure of the native rat liver arginase trimer[4] as a search probe. Iterative rounds of model building and refinement were performed using O and CNS, respectively.[27,28] Strict noncrystallographic symmetry was employed at the beginning of refinement and later relaxed to appropriately weighted constraints as judged by R_{free}. The AOH molecule was built into a simulated annealing omit electron density map in the final stages of refinement. It was clear at this point that AOH bound to arginase as the hydrated aldehyde, i.e., a gem-diol. Final refinement statistics are reported in Table 1. Figures were generated using BOBSCRIPT and Raster3D.[29,30] The atomic coordinates of the BPA−arginase I−AOH complex have been deposited in the Protein Databank (http://www.rcsb.org/pdb) with accession code 1T5F.

Results

Amino Acid Aldehydes. The methodology for the synthesis of α-amino acid aldehydes was based on a synthetic strategy utilizing the commercially available L-glutamic acid derivative, *N-t*-boc-L-glutamic acid-α-*tert*-butyl ester (Sigma), from which (*S*)-1-(*tert*-butyl-2-[bis(*tert*-butoxycarbonyl)amino]-5-oxopentanoate **1** was prepared as described.[31] For the synthesis of (*S*)-2-amino-7-oxoheptanoic acid (AOH; **5**, Scheme 1), elongation of aldehyde **1** using methyl(triphenylphosphoranylidene)acetate under Wittig conditions[32,33] provided the unsaturated ester **2** with complete (*E*)-selectivity in 79% yield. The hydrogenation of the double bond in ester **2** over Pd/C in ethyl acetate afforded the saturated ester **3** in 95% yield. Careful reduction of **3** with DIBAL-H (1.5 equiv, −78 °C, 45 min) afforded the aldehyde **4** in 95% yield. Subsequent deprotection with trifluoroacetic acid yielded (*S*)-2-amino-7-oxoheptanoic acid (AOH) **5** in 63% yield.

Given the high degree of (*E*)-stereoselectivity obtained in the synthesis of unsaturated ester **2**, this compound served as a suitable precursor for the synthesis of (*S*)−(*E*)-2-amino-7-oxohept-5-enoic acid (unsaturated AOH; **8**, Scheme 2). Reduction of **2** with DIBAL-H under controlled conditions (1.2 equiv, 0 °C, 45 min)[34] afforded the corresponding allylic alcohol **6** in 77% yield. Oxidation of **6** with Dess−Martin periodinane[35] afforded the aldehyde **7** in 60% yield. Global deprotection with trifluoroacetic acid in methylene chloride[36] furnished unsaturated AOH **8** in 87% yield.

Arginase-Inhibitor Binding Affinities. Between the two amino acid aldehyde inhibitors studied, the highest affinity was measured for AOH with $K_i = 60 \pm 8$ μM against wild-type rat arginase I at pH 9.5. For unsaturated AOH, $K_i = 360 \pm 160$ μM. Accordingly, we focused our structural studies on the arginase I−AOH complex.

Structure of the Arginase I−AOH Complex. The binding of AOH does not trigger any major changes in the tertiary or quaternary structure of BPA−arginase I, and the rms deviation of 314 monomer C_α atoms between the enzyme−inhibitor complex and the native enzyme is 0.09 Å. An electron density map is found in Figure 2a, which conclusively reveals the binding of the tetrahedral gem-diol form, rather than the native

(22) Cama, E.; Pethe, S.; Boucher, J.-L.; Han, S.; Emig, F. A.; Ash, D. E.; Viola, R. E.; Mansuy, D.; Christianson, D. W. *Biochemistry* **2004**, *43*, 8987−8999.
(23) Kanyo, Z. F.; Chen, C.-Y.; Daghigh, F.; Ash, D. E.; Christianson, D. W. *J. Mol. Biol.* **1992**, *224*, 1175−1177.
(24) Otwinowski, Z.; Minor, W. *Methods Enzymol.* **1997**, *276*, 307−326.
(25) Navaza, J. *Acta Crystallogr.* **1994**, *A50*, 157−163.
(26) Collaborative Computational Project, No. 4. *Acta Crystallogr.* **1994**, *D50*, 760−763.
(27) Jones, T. A.; Zou, J.-Y.; Cowan, S. W.; Kjeldgaard, M. *Acta Crystallogr.* **1991**, *A47*, 110−119.
(28) Brünger, A. T.; Adams, P. D.; Clore, G. M.; DeLano, W. L.; Gros, P.; Grosse-Kunstleve, R. W.; Jiang, J.-S.; Kuszewski, J.; Nilges, M.; Pannu, N. S.; Read, R. J.; Rice, L. M.; Simonson, T.; Warren, G. L. *Acta Crystallogr.* **1998**, *D54*, 905−921.
(29) Esnouf, R. M. *J. Mol. Graphics* **1997**, *15*, 132−134.
(30) Merritt, E. A.; Bacon, D. J. *Methods Enzymol.* **1997**, *277*, 505−524.
(31) Adamczyk, M.; Johnson, D. D.; Reddy, R. E. *Tetrahedron: Asymmetry* **1999**, *10*, 775−781.
(32) Kokotos, G.; Padrón, J. M.; Martín, T.; Gibbons, W. A.; Martín, V. S. *J. Org. Chem.* **1998**, *63*, 3741−3744.
(33) Padrón, J. M.; Kokotos, G.; Martín, T.; Markidis, T.; Gibbons, W. A.; Martín, V. S. *Tetrahedron: Asymmetry* **1998**, *9*, 3381−3394.
(34) Martín, R.; Islas, G.; Moyano, A.; Pericàs, M. A.; Riera, A. *Tetrahedron* **2001**, *57*, 6367−6374.
(35) Samano, V.; Robins, M. J. *J. Org. Chem.* **1990**, *55*, 5186−5188.
(36) Ellison, R. A.; Lukenbach, E. R.; Chiu, C. *Tetrahedron Lett.* **1975**, *15*, 499−502.

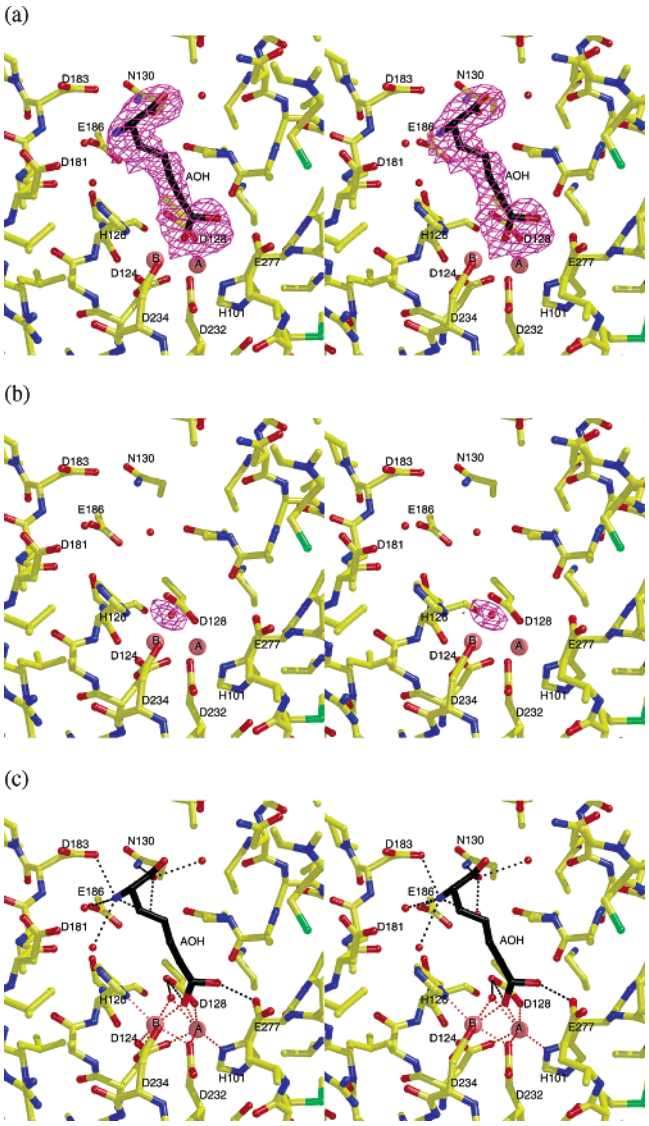

Figure 2. Simulated annealing omit electron density maps of the arginase I−AOH complex (The carbon skeleton of AOH is black): (a) AOH omitted from the structure factor calculation (contoured at 6.5σ), the partial-occupancy metal-bridging solvent molecule is not shown for clarity; (b) metal-bridging solvent molecule omitted from the structure factor calculation (contoured at 5.1σ), AOH is not shown for clarity. (c) Selected intermolecular interactions in the arginase I−AOH complex. Hydrogen bonds are indicated by black dashed lines, and metal coordination interactions are indicated by magenta dashed lines. Hydroxyl group O1 bridges $Mn^{2+}{}_A$ and $Mn^{2+}{}_B$ and hydroxyl group O2 donates a hydrogen bond to E277.

trigonal planar aldehyde form, of AOH. The $Mn^{2+}{}_A-Mn^{2+}{}_B$ separation is 3.3 Å; $Mn^{2+}{}_A$ is coordinated by H101 (Nδ1), D124 (Oδ1), D232 (Oδ2), D128 (Oδ1), and AOH hydroxyl group O1 with distorted square pyramidal geometry, while $Mn^{2+}{}_B$ is coordinated by D124 (Oδ2), H126 (Nδ1), D232 (Oδ1), D234 (Oδ1 and Oδ2), and AOH hydroxyl group O1 with distorted octahedral geometry. Hydroxyl group O1 asymmetrically bridges the metal cluster with $Mn^{2+}{}_A-O$ and $Mn^{2+}{}_B-O$ distances of 2.0 and 2.4 Å, respectively, and donates a hydrogen bond to D128. Hydroxyl group O2 is within hydrogen-bonding distance to E277 Oϵ2 (2.8 Å) and the backbone carbonyl group of A141 (3.1 Å). The $Mn^{2+}{}_A-O2$ separation is 3.2 Å, which is too long to be considered an inner-sphere metal coordination interaction. All interactions between the hydrated AOH aldehyde and arginase, apart from the interactions of hydroxyl group O2, are comparable to those observed in the binding of hydrated boronic acid inhibitors to rat arginase I and human arginase II.[8,12,13]

The average *B* factor of 48 Å^2 for AOH is much higher than that of 31 Å^2 measured for all protein atoms, which likely reflects partial occupancy inhibitor binding. If the thermal *B* factors of AOH atoms are held fixed at 31 Å^2 during occupancy refinement, the AOH occupancy refines to 80%. Consistent with partial occupancy binding of AOH, a difference electron density map reveals a residual electron density peak (~50% occupancy) refined as the metal-bridging hydroxide ion of the native enzyme (Figure 2b). It is interesting that hydroxyl group O1 of AOH, which bridges $Mn^{2+}{}_A$ and $Mn^{2+}{}_B$, is ~0.5 Å away from the position of the metal-bridging hydroxide ion in the native enzyme, suggesting some distortion of the metal coordination polyhedron as the metal-bridging hydroxide ion attacks the electrophilic carbonyl group of the inhibitor.

The α-amino group of AOH donates hydrogen bonds to D183, E186, and two solvent molecules. One of these solvent molecules forms additional hydrogen bonds with E183, N130, and the backbone carbonyl of G142, and the other solvent molecule donates hydrogen bonds to the side chain and backbone carbonyl of D181. One of the α-carboxylate oxygens accepts a hydrogen bond from the side chain of N130 and two solvent molecules, while the other α-carboxylate oxygen is not observed to engage in any hydrogen-bond interactions. These arginase−AOH interactions are comparable to those observed for the binding of amino acid boronate[12,13] and amino acid sulfonamide[10] inhibitors, except for the lack of a hydrogen-bond interaction between the α-carboxylate group and the side chain of S137 observed in complexes with the amino acid boronate inhibitors.[12,13] Intermolecular inhibitor interactions are illustrated in Figure 2c.

Discussion

The X-ray crystal structure of the BPA−arginase I−AOH complex conclusively reveals the preferential binding of AOH as the hydrated aldehyde (gem-diol) rather than the intact aldehyde. Accordingly, AOH is a reactive substrate analogue that undergoes a chemical transformation to mimic the more tightly bound tetrahedral intermediate and its flanking transition states in the arginase mechanism. That this chemical transformation—the nucleophilic attack of solvent at the electrophilic aldehyde carbonyl—is identical to that of the first step of the arginase mechanism (Figure 1) leads us to classify AOH as a new type of reaction coordinate analogue inhibitor of arginase (Figure 3).

The aldehyde moiety is sufficiently electrophilic that in aqueous solution it exists in rapid equilibrium with a substantial concentration of its hydrated gem-diol form. For example, the equilibrium constant for acetaldehyde hydration in dilute D_2O solution is 1.38, indicating a mixture of 58% gem-diol and 42% intact aldehyde.[37] Accordingly, it is possible that the preformed gem-diol form of AOH binds to the arginase I active site rather than the enzyme itself catalyzing the hydration of the AOH aldehyde moiety. There is precedent in the metalloenzyme literature for either possibility. The zinc metalloenzyme carbonic anhydrase II catalyzes the hydration of aldehyde substrates,[38] so it is conceivable that arginase I similarly catalyzes the

(37) Lewis, C. A.; Wolfenden, R. *Biochemistry* **1977**, *16*, 4886−4890.
(38) Pocker, Y.; Sarkanen, S. *Adv. Enzymol.* **1978**, *47*, 149−274.

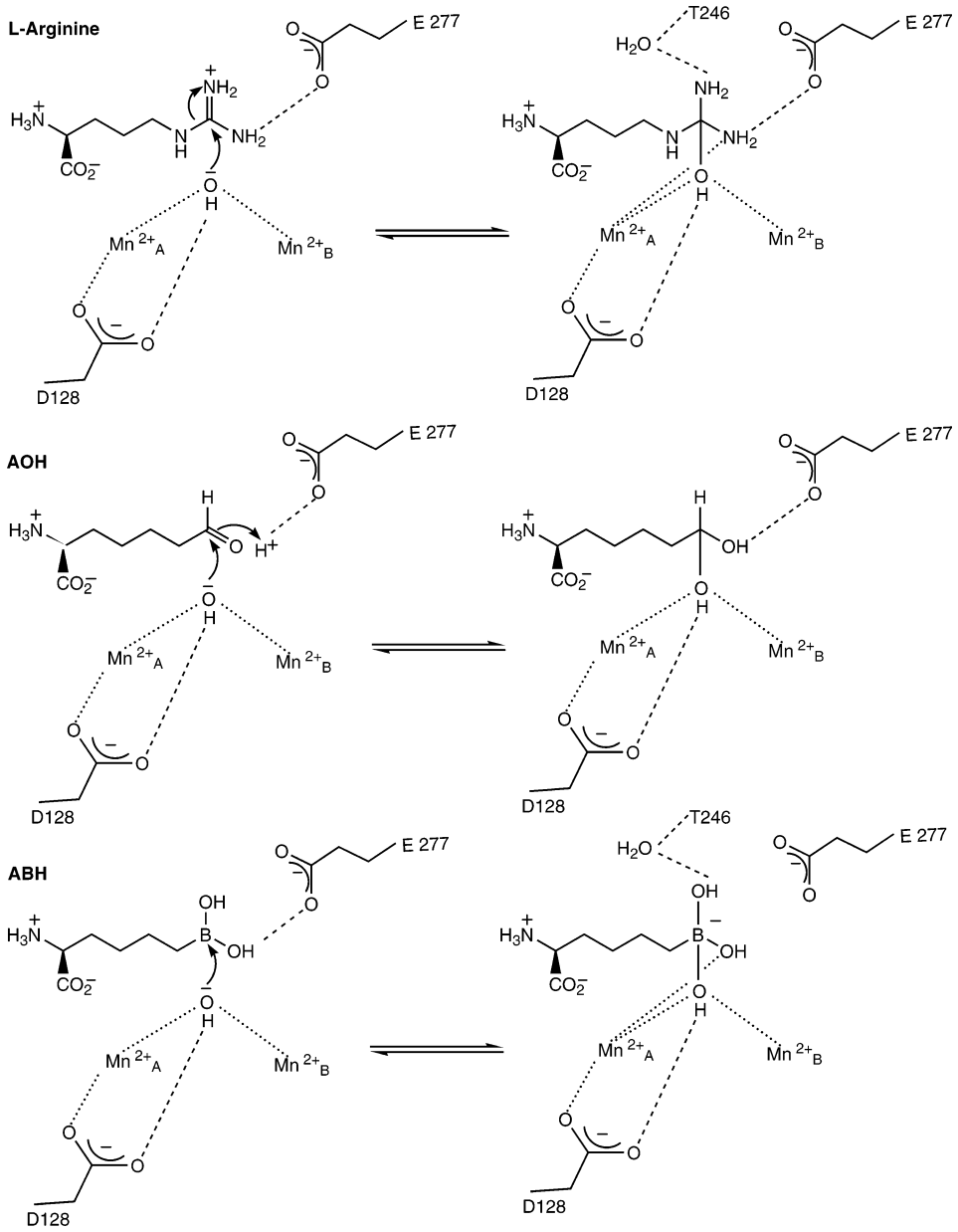

Figure 3. Reactive substrate analogue inhibitors of arginase, AOH and 2(*S*)-amino-6-boronohexanoic acid (ABH), undergo a hydration reaction presumed to mimic the first step of arginase catalysis, the hydration of the L-arginine guanidinium group. Since these inhibitors mimic the structures and the chemistry of the first step of catalysis, they are designated "reaction coordinate analogue" inhibitors. The X-ray crystal structure of the arginase I−AOH complex provides the first structural evidence that active-site residue E277 can stabilize the tetrahedral intermediate with a hydrogen-bond interaction. Note the bidentate coordination interaction of the tetrahedral intermediate in catalysis with $Mn^{2+}{}_A$, which is mimicked by the binding of ABH but not AOH. This interaction cannot occur in the precatalytic Michaelis complex since the sp^3 lone electron pair on the former guanidinium nitrogen is fully developed only when the tetrahedral intermediate is fully formed; in the substrate, this lone electron pair is delocalized in the "Y"-shaped guanidinium π system.

hydration of the reaction coordinate analogue AOH. On the other hand, the K_i value of leucine aldehyde against leucine aminopeptidase, a binuclear metalloprotease, is insensitive to deuterium substitution in the aldehyde functionality, suggesting that the preformed gem-diol form of the inhibitor is selected for binding to the enzyme.[17] Regardless of the locus of the AOH hydration reaction, that AOH binds to the arginase I active site exclusively as the tetrahedral gem-diol reflects the preferential binding of a transition-state-like structure. This result implies that transition-state stabilization by the binuclear manganese cluster makes a significant contribution to arginase catalysis.

An important new result regarding transition-state binding is evident in the arginase I−AOH complex: AOH hydroxyl group O2 (which does not coordinate to metal) donates a hydrogen bond to the carboxylate group of E277 (O···O separation = 2.8 Å). This structural feature suggests that E277 participates in transition-state stabilization just as it participates in substrate L-arginine binding to a deactivated bacterial arginase.[6] The role of E277 in binding the substrate and tetrahedral intermediate was first proposed based on analysis of the structure of native arginase I.[4] Interactions with E277 in arginase I complexes with hydrated boronic acids[12,13] are too long to be considered bona fide hydrogen bonds (O···O separations = 3.3−3.4 Å), possibly indicative of electrostatic repulsion between the negatively charged E277 carboxylate group and the negatively charged boronate anion of the inhibitor. Such electrostatic repulsion does not occur between E277 and the neutral gem-diol of the AOH hydrate, so the hydrogen bond between E277 and the tetrahedral

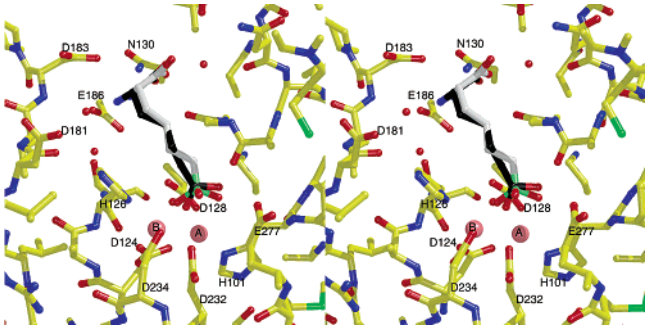

Figure 4. Superposition of the arginase I−AOH complex (AOH has a black carbon skeleton) and the binding conformation of ABH (light gray carbon skeleton with pale green boron atom) in the arginase I−ABH complex.

gem-diol is more easily formed. Importantly, the arginase I−AOH complex provides the first view of a neutral tetrahedral moiety that more faithfully mimics the neutral tetrahedral intermediate in the arginase mechanism (Figure 3).

Given the general similarities in the binding modes of AOH and its boronic acid isostere, 2(*S*)-amino-6-boronohexanoic acid (ABH),[11] as summarized in Figure 3, it is curious as to why AOH binds 600-fold more weakly than ABH. Affinity differences may arise from two subtle differences in the interactions of the tetrahedral functional group of each inhibitor. First, superposition of the AOH and ABH binding conformations in the arginase I active site (Figure 4) shows that although hydroxyl group O1 of each inhibitor bridges $Mn^{2+}{}_A$ and $Mn^{2+}{}_B$ with $Mn^{2+}\cdots O$ separations of 2.0−2.4 Å, the gem-diol of AOH is "tilted" relative to the boronate anion of ABH such that hydroxyl group O2 of ABH coordinates to $Mn^{2+}{}_A$ (2.4 Å) but hydroxyl group O2 of AOH does not coordinate to $Mn^{2+}{}_A$ (3.2 Å). In other words, the boronate anion of ABH makes a favorable bidentate coordination interaction with $Mn^{2+}{}_A$ via hydroxyl groups O1 and O2, whereas the gem-diol of AOH makes only a monodentate coordination interaction with $Mn^{2+}{}_A$ through hydroxyl group O1. Second, the O3 hydroxyl group of ABH makes a water-mediated hydrogen-bond interaction with T246,[13] but a comparable interaction cannot occur in the arginase I−AOH complex due to the presence of the aldehyde hydrogen atom at the corresponding position of the gem-diol (Figure 3).

Concluding Remarks

That arginase I−AOH affinity is in the micromolar range is consistent with structure−activity relationships outlined by Mansuy and colleagues for N^{ϵ}-hydroxy-L-lysine (K_i = 90 μM at pH 9.0; K_i = 4 μM at pH 7.4), which is isosteric with the gem-diol form of AOH less one hydroxyl group.[39] Although a crystal structure of the arginase I−N^{ϵ}-hydroxy-L-lysine complex is unavailable, the inhibitor hydroxyl group likely bridges $Mn^{2+}{}_A$ and $Mn^{2+}{}_B$ in a manner similar to that of the AOH O1 hydroxyl group, making only a monodentate metal coordination interaction. An overview of the binding modes of all tetrahedral transition-state analogue inhibitors, including amino acid sulfonamides,[10] boronic acids,[11−13,22,40] and AOH (Figure 2), suggests that the tightest binding inhibitors make bidentate coordination interactions with the binuclear manganese cluster: one atom of the tetrahedral "warhead" bridges $Mn^{2+}{}_A$ and $Mn^{2+}{}_B$, and another atom coordinates to a second site on $Mn^{2+}{}_A$ (Figure 3). Coordination to the second site on $Mn^{2+}{}_A$ therefore plays an important role in the stabilization of transition-state analogue binding; likewise, coordination to the second site on $Mn^{2+}{}_A$ must play an important role in the stabilization of the tetrahedral transition state in catalysis. With $Mn^{2+}{}_A$ and $Mn^{2+}{}_B$ responsible for activating the bridging hydroxide nucleophile, $Mn^{2+}{}_A$ responsible for bidentate coordination by the transition state, and $Mn^{2+}{}_B$ responsible for monodentate coordination by the transition state, the structural and functional requirement for two metal ions in arginase I catalysis is now clarified.

Acknowledgment. We thank Prof. David Ash for scientific discussions as well as the generous gift of recombinant rat arginase I. This work was supported by National Institutes of Health Grant GM49758 to D.W.C. E.C. was supported in part by the U.S. Army Medical Research and Materiel Command's Office of the Congressionally Directed Medical Research Programs through a Department of Defense Breast Cancer Research Predoctoral Fellowship.

JA047788W

(39) Custot, J.; Boucher, J.-L.; Vadon, S.; Guedes, C.; Dijols, S.; Delaforge, M.; Mansuy, D. *J. Biol. Inorg. Chem.* **1996**, *1*, 73−82.
(40) Collet, S.; Carreaux, F.; Boucher, J.-L.; Pethe, S.; Lepoivre, M.; Danion-Bougot, R.; Danion, D. *J. Chem. Soc., Perkin Trans.* **2000**, *1*, 177−182.